Synthesis, Structure, and Magnetic Properties of $NaTiO_2$

S. J. Clarke,[†] A. J. Fowkes,[†] A. Harrison,[‡] R. M. Ibberson,*[,§] and M. J. Rosseinsky*[,†]

Inorganic Chemistry Laboratory, University of Oxford, South Parks Road, Oxford OX1 3QR, U.K.; Department of Chemistry, University of Edinburgh, The King's Buildings, West Mains Road, Edinburgh EH9 3JJ, U.K.; and ISIS Facility, Rutherford Appleton Laboratory, Chilton, Oxon OX11 0QX, U.K.

Received July 29, 1997. Revised Manuscript Received October 16, 1997[⊗]

Details of the synthesis and structural and physical characterization of oxides with the nominal composition $NaTiO_2$ are presented. The highest sodium loading we have achieved is $Na_{0.99(2)}TiO_2$ determined using diffraction methods. The results are not consistent with a localized moment d^1 system. High-resolution neutron diffraction shows that the transition observed previously between 200 and 250 K in the magnetic susceptibility has a structural, rather than purely magnetic, origin. At room temperature $Na_{0.99(2)}TiO_2$ has the α-$NaFeO_2$ structure, space group $R\bar{3}m$ (No. 166), with the hexagonal lattice parameters $a = 3.04537(1)$ Å, $c = 16.26210(4)$ Å, and $Z = 3$. On cooling, a continuous, broad, nonhysteretic transition to a monoclinic phase occurs at about 250 K. Between 220 and 250 K, the two phases coexist, the precise temperature range of coexistence being correlated with the width of the Bragg reflections in different samples. At 5 K the monoclinic structure adopts the space group $C2/m$ (No. 12) with $a = 5.24555(6)$ Å, $b = 3.02983(3)$ Å, $c = 5.73078(6)$ Å, $\beta = 108.536(2)°$, and $Z = 2$. The structural phase transition is apparently driven by an increase in Ti−Ti bonding on cooling. This leads to small differences in band structure above and below the transition which accounts for the room-temperature magnetic susceptibility of 4.7×10^{-4} emu mol^{-1} almost halving between 250 and 200 K. The lowering of symmetry can be interpreted as a cooperative second-order Jahn−Teller distortion which is precipitated by the changes in Ti−Ti bonding.

Introduction

There has been much recent interest[1,2] in the experimental realization of model antiferromagnetic systems with unconventional ground states. The possibility of obtaining a resonating valence bond (RVB) ground state on geometrically frustrated lattices has been proposed by Anderson.[3,4] The conventional ground state of an antiferromagnet is the Neél state, in which each magnetic moment is aligned antiparallel to its neighbors. This state is not actually an eigenstate of the antiferromagnetic Hamiltonian because there are off-diagonal elements with excited states in which pairs of moments are exchanged. However it is usually a good approximation to the ground state of the system unless the magnetic moments are small and/or have few neighbors (both these situations lower the exchange energy). In this case the true ground state is better thought of as a superposition of the Neél state and others derived from it by interchange of pairs of moments. This has been called the RVB state, by analogy with the valence bond description of covalent bonding. It appears that the antiferromagnetic square lattice with low ($S = {}^1/_2$) moments is best described by the classical Neél model,[2,5] so attention has turned to magnetically frustrated systems in which the classical state is further destabilized with respect to the RVB state. Antiferromagnetic two-dimensional lattices based on equilateral triangles such as the triangular and Kagomé[6] lattices, and three-dimensional lattices based on regular tetrahedra, such as the pyrochlore lattice,[7] are frustrated because it is impossible to completely satisfy antiferromagnetic exchange interactions across more than two edges of each triangular plaquette simultaneously. Frustration can also arise on a square lattice with strong next-nearest-neighbor superexchange (which is topologically equivalent to the isosceles triangular lattice[8]). One of the most likely candidates for an RVB ground state is thus the triangular lattice antiferromagnet with $S = {}^1/_2$; however, there is no clear theoretical consensus regarding its behavior,[9] and, so far, it has not been realized experimentally.

[†] University of Oxford.
[‡] University of Edinburgh.
[§] Rutherford Appleton Laboratory.
[⊗] Abstract published in *Advance ACS Abstracts,* December 15, 1997.

(1) Ramirez, A. P. *Annu. Rev. Mater. Sci.* **1994**, *24*, 453.
(2) Manousakis, E. *Rev. Mod. Phys.* **1991**, *63*, 1.
(3) Anderson, P. W. *Mater. Res. Bull.* **1973**, *8*, 153.
(4) Fazekas, P.; Anderson, P. W. *Philos. Mag.* **1974**, *30*, 432.
(5) Clarke, S. J.; Harrison, A. *J. Magn. Magn. Mater.* **1995**, *140−144*, 1627.
(6) Wills, A. S.; Harrison, A. *J. Chem. Soc., Faraday Trans.* **1996**, *92*, 2161.
(7) Greedan, J. E.; Raju, N. P.; Maignan, A.; Simon, C.; Pedersen, J. S.; Niraimathi, A. M.; Gmelin, E.; Subramanian, M. A. *Phys. Rev.* **1996**, *B54*, 7189.
(8) Bramwell, S. T.; Carling, S. G.; Harding, C. J.; Harris, K. D. M.; Kariuki, B. M.; Nixon, I.; Parkin, I. P. *J. Phys.: Condens. Matter* **1996**, *8*, L123.

S0897-4756(97)00538-3 CCC: $15.00 © 1998 American Chemical Society
Published on Web 01/19/1998

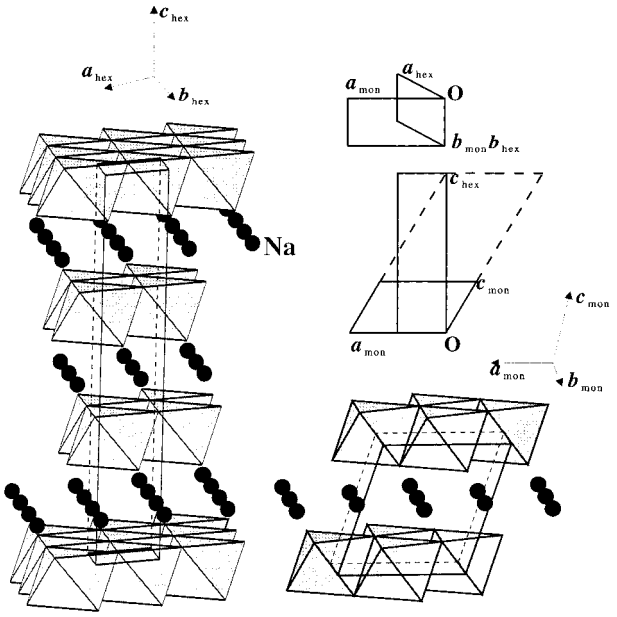

Figure 1. Structure of $NaTiO_2$. At room temperature, the space group is $R\bar{3}m$ (left). Below 250 K, the space group is $C2/m$ (right). The TiO_6 octahedra are shaded. The relationship between the trigonal and monoclinic cells is shown.

$NaTiO_2$ adopts the α-$NaFeO_2$ structure.[10] This is an ordered variant of the rock-salt structure which is particularly common in both undistorted and distorted forms in alkali metal/transition metal oxides. Layers of edge-sharing TiO_6 octahedra and edge-sharing NaO_6 octahedra alternate along the rock-salt [111] direction (i.e., there are alternating NaO and TiO slabs). The undistorted form of the structure with the space group $R\bar{3}m$ (No. 166) is shown in Figure 1, together with a common distorted form with the space group $C2/m$. The relationship between the two unit cells is also shown. In the rhombohedral form all the metal atoms are in trigonal antiprismatic (D_{3d}), rather than octahedral (O_h), coordination. The TiO_6 trigonal antiprisms are octahedra compressed along the 3-fold axis; the NaO_6 trigonal antiprisms are octahedra which have been lengthened along the 3-fold axis. $NaTiO_2$ formally contains d^1 Ti^{3+} with $S = {}^1/_2$ arranged on a triangular lattice with a separation of about 3.04 Å.

In view of the above, $NaTiO_2$ has long been regarded as a possible candidate for a triangular lattice antiferromagnet with an RVB ground state. A range of physical property measurements and interpretations has been reported for this material.[1,10−12] We show that reliable property measurements require the analysis of high-resolution diffraction data in order to correlate correctly the properties with the structure. The hexagonal lattice parameters in the space group $R\bar{3}m$ range between $a = 3.01-3.05$ Å and $c = 16.41-16.23$ Å, for samples of the same nominal composition made under broadly similar conditions. In this and a future article,[13] we show that the samples with shorter a and longer c axes are slightly deficient in Na, in agreement with investigations of known Na-deficient samples[14] with mixed $Ti^{3+/4+}$ character. This deficiency thus results in shorter intralayer Ti−Ti distances and has a profound effect on the magnetic properties, which explains the range of behavior previously reported. We also find that it affects the details of the structure. Previously,[15] we presented preliminary data focusing on the difficulty of preparing single-phase stoichiometric (i.e., $Na_{1.0}TiO_2$) material and which appeared to be at odds with the view that the material is an insulating magnet. In the current article, we concentrate on samples with compositions very close to $Na_{1.0}TiO_2$ and use high-resolution neutron powder diffraction to investigate the structure as a function of temperature and interpret the magnetic properties. We conclude that the broad transition in the susceptibility below 250 K, which has previously been observed,[11] is not due to the ordering or change in dynamics of localized moments but is instead due to small changes in the band structure of a delocalized electron system caused by a subtle structural distortion. In a separate article[13] we describe a similar analysis of material which is about 7% deficient in Na.

Experimental Section

Synthesis. Samples of $Na_{1.0}TiO_2$ were prepared using modifications, discussed below, of the following basic method. Anatase TiO_2 (Aldrich, 99.999%), which was confirmed to be phase pure using powder X-ray diffraction, was dried under vacuum at 750 °C and was then reduced with freshly cut Na (Aldrich, 99.9%) at between 950 and 1000 °C for several days in clean Ta (Plansee, 99.9%) or Fe (ARMCO, 99.8+%) tubes sealed by arc welding in a Centorr Associates arc furnace under 1 atm of clean Ar. The tubes were sealed under vacuum in quartz ampules or placed in a flow of argon to protect them from oxidation at elevated temperatures. Na and $NaTiO_2$ are both very air-sensitive, so all manipulations were carried out in a helium-filled drybox in which the atmosphere was continuously circulated so that the combined O_2 and H_2O content was less than 1 ppm. Although anatase can be partially reduced by *n*-BuLi in hexane at room temperature,[16] it was not possible to insert the larger Na using sodium naphthalide in tetrahydrofuran.

A number of samples are considered in this paper, and their syntheses are summarized in Table 1. As indicated later, the Na content is influenced by the exact method of preparation, and has a very profound effect on the structural and magnetic properties. We took various steps to avoid Na deficiency. The Na content and the extent of Na/Ti disorder were determined by the analysis of diffraction data. We could not perform chemical analysis because the materials were insoluble in concentrated nitric acid, aqua regia, and aqueous HF. Sample 1 was obtained by heating Na (0.03739(1) mol) with anatase (0.03119(1) mol), composition $Na_{1.2}TiO_2$, at 950 °C for 5 days in a 2.5 cm diameter Fe container. The black powder removed was transferred to one side of a glass H-cell,[17] and sodium-dried ammonia was condensed onto the sample to dissolve the excess Na. The Na/NH_3 solution was poured to the other side of the cell, and the procedure was repeated to wash out all of the Na. The powder was then dried under vacuum at room

(9) Yang, K.; Warman, L. K.; Girvin, S. M. *Phys. Rev. Lett.* **1993**, *70*, 2641.
(10) Hagenmuller, P.; Lecerf, A.; Onillon, M. *C. R. Acad. Sci.* **1962**, *255*, 928.
(11) Takeda, K.; Miyake, K.; Takeda, K.; Hirakawa, K. *J. Phys. Soc. Jpn.* **1992**, *61*, 2156.
(12) Hirakawa, K.; Kadowaki, H.; Ubukoshi, K. *J. Phys. Soc. Jpn.* **1985**, *54*, 3526.
(13) Clarke, S. J.; Fowkes, A. J.; Harrison, A.; Ibberson, R. M.; Rosseinsky, M. J., in preparation.
(14) Maazaz, A.; Delmas, C. *C. R. Acad. Sci.* **1982**, *295*, 759.
(15) Clarke, S. J.; Duggan, A. C.; Fowkes, A. J.; Harrison, A.; Ibberson, R. M.; Rosseinsky, M. J. *Chem. Commun.* **1996**, 409.
(16) Murphy, D. W.; Greenblatt, M.; Zahurak, S. M.; Cava, R. J.; Waszczak, J. V.; Hull, G. W.; Hutton, R. S. *Rev. Chim. Miner.* **1982**, *19*, 441.
(17) Chen, X. Z.; Dye, J. L.; Eick, H. A.; Elder, S. H.; Tsai, K.-L. *Chem. Mater.* **1997**, *9*, 1172.

Table 1. Summary of the Different Syntheses of Na_xTiO_2 Samples[a]

sample	synthesis	*a*/Å	*c*/Å	*V*/Å^3
1	1.2Na + TiO_2, 950 °C, 5 days, steel tube, washed with liquid NH_3	3.05155(3)	16.2313(1)	130.896(3)[b]
		3.04585(3)	16.2563(1)	130.608(3)[c]
2	Na + TiO_2, 1000 °C, 7 days, Ta tube, equilibrated with Na at 300 °C	3.04537(1)	16.26210(4)	130.573(1)
3	Na + TiO_2, 1000 °C, 7 days, Ta tube, equilibrated with Na at 1000 °C	3.04682(1)	16.25287(5)	130.663(1)
4	as sample 2, equilibrated twice at 300 °C	3.03550(6)	16.3119(3)	130.165(5)
5	1.4Na + TiO_2, 1000 °C, 7 days, Ta tube	3.03917(4)	16.2926(2)	130.325(4)
6	as sample 5	3.04185(2)	16.2776(1)	130.435(3)
7	as sample 4	3.04474(4)	16.2636(2)	130.571(4)
8	as sample 2	3.04476(8)	16.2630(4)	130.567(7)
A	as sample 2	3.04375(2)	16.2587(1)	130.447(2)
B	as sample 5	3.04358(3)	16.25329(2)	130.389(3)
C	Na + TiO_2, 1000 °C, 7 days, Ta tube, two grindings and reheatings at 1000 °C	3.01358(2)	16.4097(2)	129.061(2)

[a] The numbered samples were measured on HRPD and samples A, B, and C were measured on the Daresbury synchrotron station 9.1. All except sample 1 were determined to be single phase by our measurements. [b] 25(1)%. [c] 75(1)%.

temperature at about 10^{-4} Torr for several hours. Reaction of the excess Na with ethanol yielded NaOEt, which was titrated against aqueous HCl. This indicated that the stoichiometry of the solid remaining was close to $Na_{1.0}TiO_2$ and that there was no further reduction to Ti^{2+} by the excess sodium.

Samples 2 and 3 had a nominal initial composition of $Na_{1.0}TiO_2$. Sample 2 was prepared by sealing 0.01371(1) mol of Na and 0.01371(1) mol of anatase in a Ta tube and heating to 450 °C for 60 h, raising the temperature to 800 °C for 48 h, before performing a final firing at 1000 °C for 7 days, and then turning the furnace off. Black powder (1.4021 g) was removed from the tube; the slight shortfall probably being due to some product being stuck to the sides of the tube. The material was ground and then replaced in a fresh Ta tube which was not sealed; instead this Ta tube was placed at one end of a 20 cm long Pyrex tube with excess Na, contained in a Pyrex insert, at the other end. The composition in the tube was $Na_{1.0}TiO_2$ + 0.4Na. The Pyrex tube was sealed under vacuum at 10^{-5} Torr and heated for 4 days in a four-zone tube furnace with the $NaTiO_2$ at 300 °C and the Na at 290 °C in order to equilibrate the powder with Na vapor at a temperature where the vapor pressure of Na above $NaTiO_2$ is insignificant.

Sample 3 was prepared in a manner similar to that for sample 2, except that instead of performing the equilibration with Na at low temperatures, the initial $Na_{1.0}TiO_2$ was ground and then placed in a second sealed Ta tube with some additional Na, so that the composition in the tube was again $Na_{1.0}TiO_2$ + 0.4Na. This was heated at 450 °C for 3 days, then 800 °C for 2 days, and finally 1000 °C for 3 days. Excess Na had sublimed to one end of the tube at the end of the reaction.

Samples 1−3 were the subjects of detailed structural investigations using high-resolution neutron powder diffraction. Sample 2 is the least structurally complicated sample, although it may be slightly deficient in Na compared to samples 1 and 3, which show clear or incipient multiple phase behavior, respectively. Samples 4−8, prepared under slightly modified conditions and screened using neutron diffraction for phase purity and composition, are summarized in Table 1.

Powder Diffraction. X-ray diffraction experiments were carried out at room temperature using a Siemens D5000 diffractometer operating in Debye−Scherrer geometry with Cu Kα_1 radiation (1.540 51 Å) selected using a Ge(111) monochromator. A 6° linear position-sensitive detector was used with an effective step size of 0.02°. The samples were contained in 0.3 mm diameter dry glass capillary tubes to prevent aerial oxidation. The capillary was rotated continuously about its long axis during the measurement. The absorption coefficient of the sample was determined by measuring the intensity of the attenuated incident beam with and without the sample present. This was used as a constant in the Rietveld refinements in the expression for absorption given by Hewat.[18] However, the absorption was severe enough for the thermal displacement parameters for all the atoms to refine to negative values. The laboratory instrument was used to monitor sample quality and the progress of the solid-state reactions and for Rietveld refinement of sample 2.

High-resolution X-ray diffraction measurements on station 9.1 of the Synchrotron Radiation Source (SRS), Daresbury, UK, have been described previously.[15] The data were collected in the angular range 8−116° in 2θ using $\lambda = 0.9987$ Å on samples contained in 0.3 mm glass capillaries. Data were collected with a step size of 0.01° and for 1 s/point in the range 8−60°; 2 s/point 60−78°; 4 s/point 78−90°, and 5 s/point in the range 90−116°. The instrument has a $\Delta d/d$ resolution of 3.5×10^{-4} at $d = 2.2$ Å[19] compared with $\Delta d/d$ of 2×10^{-3} for the D5000 diffractometer at the same d spacing. Absorption was far less severe using the shorter wavelength X-rays.

High-resolution neutron powder diffraction was performed on samples 1−8 using the high-resolution powder diffractometer (HRPD) at the ISIS spallation source, Rutherford Appleton Laboratory. HRPD has a constant resolution $\Delta d/d = 8 \times 10^{-4}$ at the higher flux 1 m position used in these measurements. Sample 1 (2.8 g) was measured at 295 and 100 K over the range $0.4 \le d/\text{Å} \le 2.4$ for a total proton current of 135 μA. The sample was contained in a rectangular vanadium can, sealed with an indium gasket. Sample 2 (0.5 g) was measured at 5 and 300 K over the above d-spacing range for a total proton current of 600 μA, and at a series of temperatures between 180 and 300 K over the shorter window $0.9 \le d/\text{Å} \le 1.7$ for 30 min each during warming. Sample 3 (0.9 g) was measured at 300 K for $1.2 \le d/\text{Å} \le 2$ and between 190 and 290 K in the shorter window used for sample 2. The shorter window was used to improve the counting statistics and hence lattice parameter precision when the small samples were measured for a short length of time. Samples 2 and 3 were contained in 4 mm diameter cylindrical vanadium cans, sealed with In gaskets. The neutron diffraction data were not corrected for absorption because all three elements have small absorption cross sections. There was no evidence for preferred orientation. Rietveld refinement of the neutron diffraction data was carried out using the program TF12LS,[20] which contains a peak-shape description appropriate to HRPD. Refinement of the X-ray data was accomplished using the General Structure Analysis System (GSAS).[21] The other samples in Table 1 were screened briefly on HRPD in order to determine their lattice parameters and inspect their peak profiles for evidence of multiphase behavior or compositional inhomogeneities.

Magnetic Susceptibility. Measurements were performed on about 0.1 g of powder either using a Cryogenic Consultants SCU 500C SQUID magnetometer in fields of up to 6 T and between 4.2 and 325 K or using a Quantum Design MPMS-5

(18) Hewat, A. *Acta Crystallogr.* **1979**, *A35*, 248.

(19) Langford, J. I.; Cernik, R. J.; Louër, D. *J. Appl. Crystallogr.* **1991**, *24*, 913.

(20) David, W. I. F.; Ibberson, R. M.; Matthewman, J. C. *Rutherford Appleton Laboratory Report*, 1992, RAL-92-032.

(21) Larsen, A.; von Dreele, R. B. *The General Structure Analysis System*, Los Alamos National Laboratory, 1985.

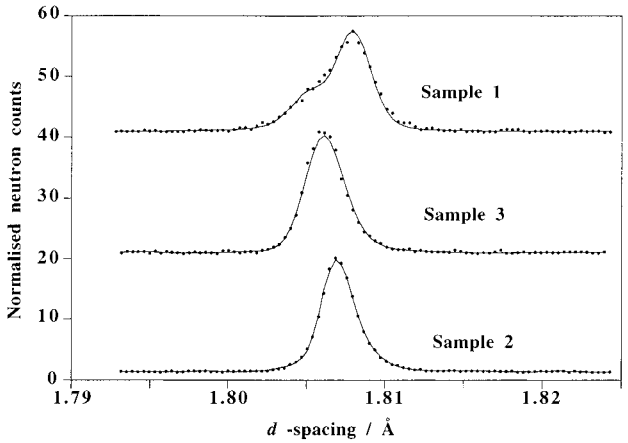

Figure 2. The {009} reflection of samples 1−3 measured on HRPD at room temperature showing the variation in sample peak widths. The lines are fits to single peaks for samples 2 and 3, and two peaks for sample 1. The three plots are offset from one another along the vertical axis for clarity.

SQUID magnetometer in fields of 1 and 2 T, and at temperatures between 5 and 330 K. The powder was contained within gelatine capsules that were sealed with Superglue within a few seconds of removal from the drybox. It was found that exposure of a nonglued capsule containing a sample to air for a few minutes could lead to a marked change in the magnetic susceptibility of the sample if the two ends of the capsule did not fit together tightly.

Electron Paramagnetic Resonance Spectroscopy (EPR). EPR measurements were carried out on about 20 mg of sample 2 between 4 and 300 K using a Varian E-Line Century Series spectrometer equipped with an Oxford Instruments He-flow cryostat.

Results

Diffraction Experiments. The lattice parameters and unit-cell volumes of samples 1−8 are given in Table 1. Sample 1, which has been discussed previously,[15] had the largest *a* and smallest *c* parameters, suggesting that it had the largest Na content,[14] but was determined to be biphasic using refinement of HRPD data. Peak shape, the criterion for phase purity, was also variable, as shown in Figure 2. Samples 2 and 3 had the largest *a* and smallest *c* of the samples that appeared to be single phase. The unit-cell volumes of the two phases in sample 1 were both slightly larger than those of samples 2 and 3. Sample 2 had the narrowest peaks; some samples were like sample 1 and clearly showed 2-phase behavior, with the peaks from the two phases partially resolved from one another. Other samples, including sample 3, had peaks that were significantly broader than those in sample 2 but that could still be described as single peaks (Figure 2). Pawley intensity extractions, which are independent of a structural model,[22] revealed that the Lorentzian contributions to the peak width of samples 2 and 3 were approximately equal, suggesting that the particle sizes are similar for the two samples. The Lorentzian contributions to the peak widths were considerably smaller than the Gaussian contributions in all cases and the Gaussian width for sample 3 was about 1.7 times that in sample 2.

More detailed discussion of the crystal structure is restricted to the single phase sample 2. At room temperature the space group is $R\bar{3}m$, and the hexagonal lattice parameters are $a = b = 3.04537(1)$ Å and $c = 16.26210(4)$ Å with $Z = 3$. Neutron and X-ray (D5000) refinements at room temperature were used to investigate the Na:Ti ratio. The neutron refinement is shown in Figure 3. O has the largest neutron scattering length of the three elements (5.8 fm) and Ti has a negative neutron scattering length (−3.4 fm) roughly equal in magnitude to that of Na (3.6 fm). This is in great contrast to the differences in X-ray scattering factors. In principle the method of joint refinement should be able to determine the stoichiometry and any degree of site disorder more accurately and precisely than either method on its own in this case. However, the effect of the much slower falloff in atomic scattering factor with decreasing *d* spacing for neutrons compared to X-rays weighted the neutron data much more heavily than the X-ray data in a joint refinement. Furthermore, the transmission geometry employed in the X-ray experiment in order to exclude air resulted in large absorption by the sample that could not be fully corrected for and resulted in unreliable thermal displacement parameters for the atoms. We thus used the two measurements independently to elucidate the structural details.

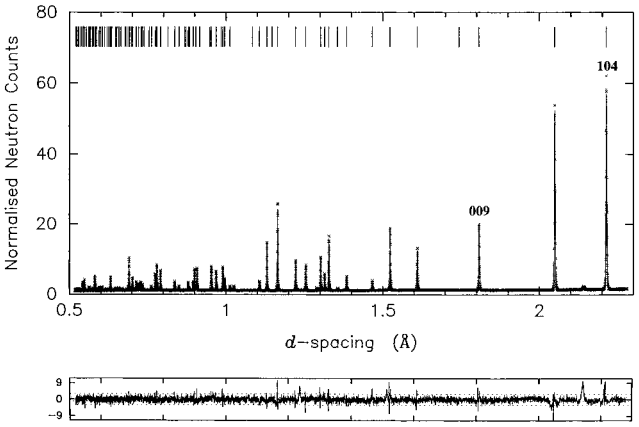

Figure 3. Results of Rietveld refinement of high-resolution neutron diffraction data for sample 2 at room temperature (rhombohedral).

The refined parameters for sample 2 are presented in Table 2. As well as slight nonstoichiometry, there is the possibility of disorder between the Na and Ti sites. This is a similar situation to that encountered by Reimers et al. in the refinement of $Li_xNi_{2-x}O_2$ ($x \approx 1$).[23] Initially, we refined the disorder between the Na and Ti sites and a thermal parameter for each different site with the composition fixed at $Na_{1.0}TiO_2$. These refinements are summarized in Table 2 and indicated that there was a mean disorder between the Na and Ti sites of 4.6(5)%. The use, in the neutron refinement, of anisotropic displacement parameters for O did not improve the fit significantly, indicating that the atom was approximately isotropic. Like Reimers et al., we found that the isotropic thermal displacement parameters were very strongly correlated (from 60 to 80%) with the site occupancies. In a second series of refinements, an overall thermal parameter was used, which was not strongly correlated with any of the site oc-

(22) Pawley, G. S. *J. Appl. Crystallogr.* **1981**, *14*, 357.

(23) Reimers, J. N.; Dahn, J. R.; Greedan, J. E.; Stager, C. V.; Liu, G.; Davidson, I.; Vonsachen, U. *J. Solid State Chem.* **1993**, *102*, 542.

Table 2. Structural Parameters for the High- and Low-Temperature Phases of $NaTiO_2$ Obtained by Rietveld Refinement of High-Resolution Neutron Powder Diffraction Data and Laboratory X-ray Diffraction Data Collected on Sample 2 ($Na_{0.99(2)}TiO_2$) at 298 and 5 K

	temp/K		
	298	298	5
instrument	HRPD	D5000	HRPD
space group	$R\bar{3}m$ (No. 166)	$R\bar{3}m$ (No. 166)	$C2/m$ (No. 12)
a/Å	3.04537(1)	3.04295(8)	5.24555(6)
b/Å	3.04537(1)	3.04295(8)	3.02983(3)
c/Å	16.26210(4)	16.2580(4)	5.73078(6)
α/deg	90	90	90
β/deg	90	90	108.536(2)
γ/deg	120	120	90
V/Å^3	130.613(1)	130.373(7)	86.355(2)
ρ_{calc}/g cm^{-3}	3.91481(4)	3.9220(3)	3.9475(1)
Z	3	3	2
xyz_{Na}	3*a*: (0, 0, 0)	3*a*: (0, 0, 0)	2*a*: (0, 0, 0)
xyz_{Ti}	3*b*: (0, 0, $^1/_2$)	3*b*: (0, 0, $^1/_2$)	2*d*: (0, $^1/_2$, $^1/_2$)
xyz_O	6*c*: (0, 0, 0.23479(2))	6*c*: (0, 0, 0.2346(2))	4*i*: (0.7702(2), 0, 0.2939(3))
U_{Na}/Å^2	0.0080(2)	−0.021(1)[a]	0.0048(6)
U_{Ti}/Å^2	0.0055(2)	−0.036(2)[a]	0.0066(7)
U_O/Å^2	0.0097(2)	−0.033(2)[a]	0.011(1)
Na/Ti disorder/%	3.8(2)	5.3(8)	4.7(6)
R_p	0.0350	0.0151	0.114
wR_p	0.0393	0.0214	0.114
χ^2	2.13	1.02	1.82

[a] Negative and large due to the effects of absorption in transmission geometry.

cupancies. In treating the neutron diffraction data in this way, we constrained the Ti:O ratio to be 1:2, and the Ti layers to be filled in order to reduce the number of parameters. We were then able to refine the disorder between the Na and Ti sites *and* the occupancy of Na in the Na site. This produced the composition $Na_{0.985(5)}TiO_2$ and a disorder of 1.9(1)%. The goodness of fit was slightly poorer ($\chi^2 = 2.26$ vs 2.13) than in the first series of refinements in which there were more variables. In the refinement of the X-ray data collected on our laboratory D5000, we found that the correlation between the overall thermal parameter and the occupancy of the Na site was too large to enable the Na site occupancy to be refined, so we were able only to determine a value for the disorder which was 2(1)% and thus somewhat lower than the value obtained when a different thermal parameter was allowed for each site. However, the results for the degree of disorder from the four different refinements are all broadly in agreement with each other. The statistical precision in the disorder and the stoichiometry are underestimates of the accuracy with which we can determine these quantities, so we conclude from our room-temperature data that the composition is $Na_{0.99(2)}TiO_2$ and the disorder is 3.5 ± 1.5%. Results of the neutron and X-ray refinements at 298 K are listed in Table 2. The site disorder does appear to be real, and its incorporation into the refinement did improve the goodness of fit significantly, reducing χ^2 from 2.30 to 2.13.

Having defined the room-temperature structure of the single-phase sample, we attempted to establish the differences between the two phases present in sample 1. The difference in the lattice parameters and unit-cell volumes suggests that phase 1, which constitutes about 25% of the sample, is richer in Na by up to 1.5% than phase 2, which constitutes the remainder. Alternatively, some or all of the difference could be due to different degrees of disorder between the Na and Ti layers. We used the MULTI version of the TF12LS software to refine the two rhombohedral phases present,

Table 3. Results of Rietveld Refinement of the Two Rhombohedral Phases Present in Sample 1 at 298 K

	phase	
	1	2
a/Å	3.05414(4)	3.04846(2)
c/Å	16.2412(2)	16.26903(9)
V/Å^3	131.198(3)	130.934(1)
phase fraction	0.258(8)	0.742(8)
z_o	0.2340(2)	0.23476(7)
U/Å^2	0.0056(1)[a]	0.0056(1)[a]
disorder/%	1.6(7)	3.3(3)

[a] Constrained equal in both phases. $\chi^2 = 2.49$; $R_p = 0.0817$; $wR_p = 0.0968$.

with a single thermal parameter for the whole pattern to avoid large correlations between thermal parameters and occupancies or disorder. We initially constrained the compositions of the two phases to both be $Na_{1.0}TiO_2$. We then refined the relative phase fractions, the atomic coordinates, the overall temperature factor, independent profile parameters, and the degree of disorder present in the two phases. The results are summarized in Table 3. We found that the overall thermal parameters for each phase could be refined independently without significantly affecting the other parameters or giving rise to significant statistical correlation with other parameters, although the values differed by 60%.

If the Na contents of the two phases were varied independently, there was a slight increase in χ^2 and the two compositions were $Na_{1.025(9)}TiO_2$ (25.2%) and $Na_{0.956(5)}TiO_2$ (74.8%) with disorders of 2.8(7)% and 2.2(3)%, respectively. These differences in composition seem unreasonably large compared with our results, summarized below, relating differences in unit-cell volume to differences in Na content. Neither the degree of disorder nor the Na occupancy were strongly correlated with the phase fractions.

Our refinements do not clearly show how the two phases in sample 1 differ. There is some evidence that they differ in the degree of disorder between the Na and Ti sites, although the difference is barely significant at

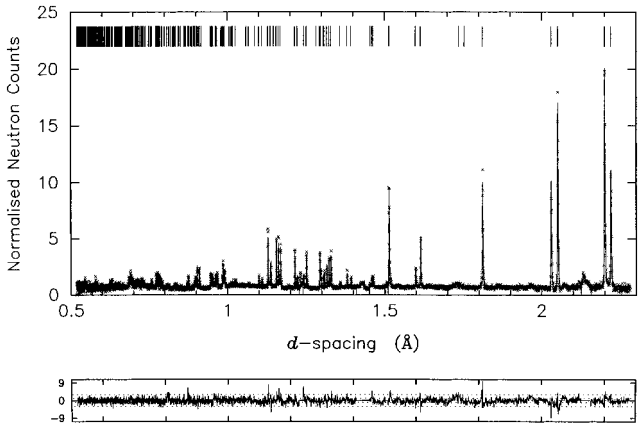

Figure 4. Results of Rietveld refinement of high-resolution neutron diffraction data for sample 2 at 5 K (monoclinic). Some regions were excluded from the refinement because they contained weak diffraction peaks arising from the vanadium sample can and from the cryostat.

the 3σ level. It is unlikely that they differ considerably in overall composition, although this combined with differences in disorder could be responsible for the presence of two phases.

In high-resolution neutron diffraction patterns measured on single-phase sample 2 below the magnetic transition, some of the peaks were clearly split. This can clearly be seen in Figure 4: the rhombohedral {009} reflection is unsplit, but the intense {104} reflection is clearly split. $\Delta d/d$ for the split reflections is 4×10^{-2}, so the two peaks would be at least partially resolved on most diffraction instruments. Rietveld refinement shown in Figure 4, and summarized in Table 2, confirmed that sample 2 was a single monoclinic phase, adopting the space group $C2/m$. The lattice vectors of the two cells are related according to $\boldsymbol{a}_{\mathbf{mon}} = 2\boldsymbol{a}_{\mathbf{hex}} + \boldsymbol{b}_{\mathbf{hex}}$; $\boldsymbol{b}_{\mathbf{mon}} = \boldsymbol{b}_{\mathbf{hex}}$; $\boldsymbol{c}_{\mathbf{mon}} = {}^1/_3(\boldsymbol{c}_{\mathbf{hex}} - 2\boldsymbol{a}_{\mathbf{hex}} - \boldsymbol{b}_{\mathbf{hex}})$, so that $b_{\mathrm{mon}} = a_{\mathrm{hex}} = a_{\mathrm{mon}}/\sqrt{3}$ and $c_{\mathrm{mon}} = {}^1/_3 c_{\mathrm{hex}} \sin\beta$. This is shown diagramatically in Figure 1. At 5 K the lattice parameters were $a = 5.24555(6)$ Å, $b = 3.02983(3)$ Å, $c = 5.73078(6)$ Å, and $\beta = 108.536(2)°$. There were no measurable superlattice reflections, so the primitive unit cell has the same volume above and below the transition. The degree of disorder at 5 K was determined to be 3.5(5)%, irrespective of whether individual thermal parameters or an overall thermal parameter were used, which agrees with the value at room temperature. At temperatures between 220 and 250 K, i.e., within the region of the transition in the magnetic susceptibility, the rhombohedral and monoclinic phases coexist. Resolution of the two coexisting phases is possible because of the high resolution of HRPD. Simultaneous Rietveld refinement of both phases in the transition region was carried out using the MULTI version of the TF12LS software. The result of the refinement at 245 K where the two phases are present in approximately equal amounts is shown in Figure 5. Figure 5 also shows the relative proportions of the two phases, determined by Rietveld refinement, at each temperature.

Consider the behavior on cooling through the transition. The evolution of the Ti−Ti distances, which equate to a_{hex} in the rhombohedral phase and b_{mon} and $(\sqrt{a_{\mathrm{mon}}^2+b_{\mathrm{mon}}^2})/2$ in the monoclinic phase and are thus

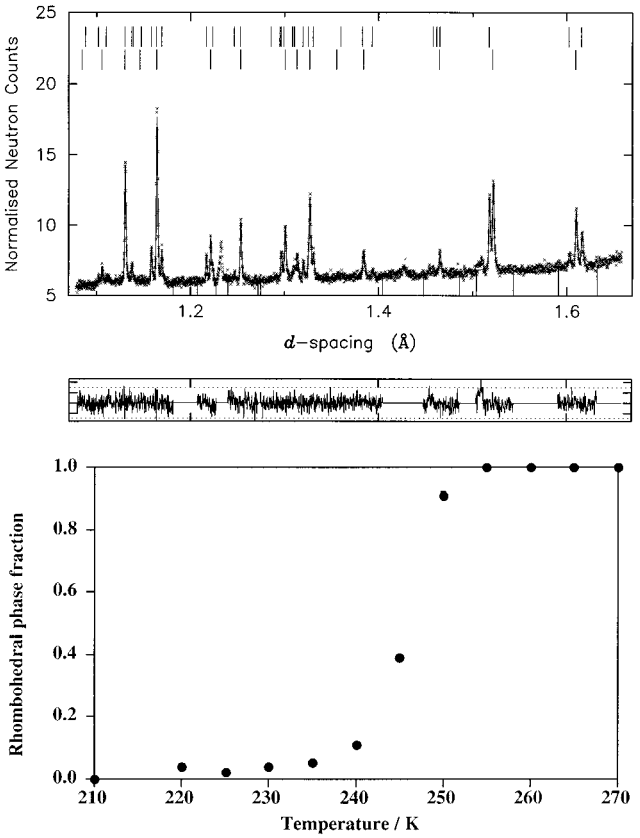

Figure 5. Results of two-phase Rietveld refinement of high-resolution neutron diffraction data for sample 2 at 245 K. 39(1)% of the sample is rhombohedral and 61(1)% is monoclinic. Some regions were excluded from the refinement because they contained weak diffraction peaks arising from the vanadium sample can and from the cryostat. Bottom: proportion of the rhombohedral and monoclinic phases as a function of temperature as determined by Rietveld refinement. (the error bars lie within the points).

particularly well-defined, is shown in Figure 6a. There is an abrupt shortening, by about 0.3%, of the Ti−Ti distance as the monoclinic structure is adopted. The apparent upturn in a_{hex} in the region of coexistence is not significant at the 3σ level because of the small amount of rhombohedral phase present at those temperatures. The behavior of the average interlayer separation given by c_{hex} and $3c_{\mathrm{mon}} \sin\beta_{\mathrm{mon}}$ is shown in Figure 6b. There is an abrupt increase in the interlayer separation at the rhombohedral-to-monoclinic transition which is the sum of an expansion, in this direction, of the TiO slabs and a slight contraction of the NaO slabs. The volume of the primitive unit cell, plotted as a function of temperature in Figure 6c, shows an abrupt contraction as the structure becomes monoclinic, although the weighted mean volume undergoes a much smoother change. The volume change is dominated by the contraction in the Ti−Ti distance and augmented by the contraction in the NaO slabs, although these are opposed by the expansion in the c direction of the TiO slabs. At 245 K, the temperature considered in Figure 5, 39(1)% of sample 2, was rhombohedral, and the Ti−Ti distance was 3.04242(5) Å. The two Ti−Ti distances in the monoclinic phase at 245 K were 3.0348(1) and 3.0343(1) Å. The abrupt shortening of the Ti−Ti distance on cooling seems to drive the distortion to lower symmetry. These results indicate that the structural

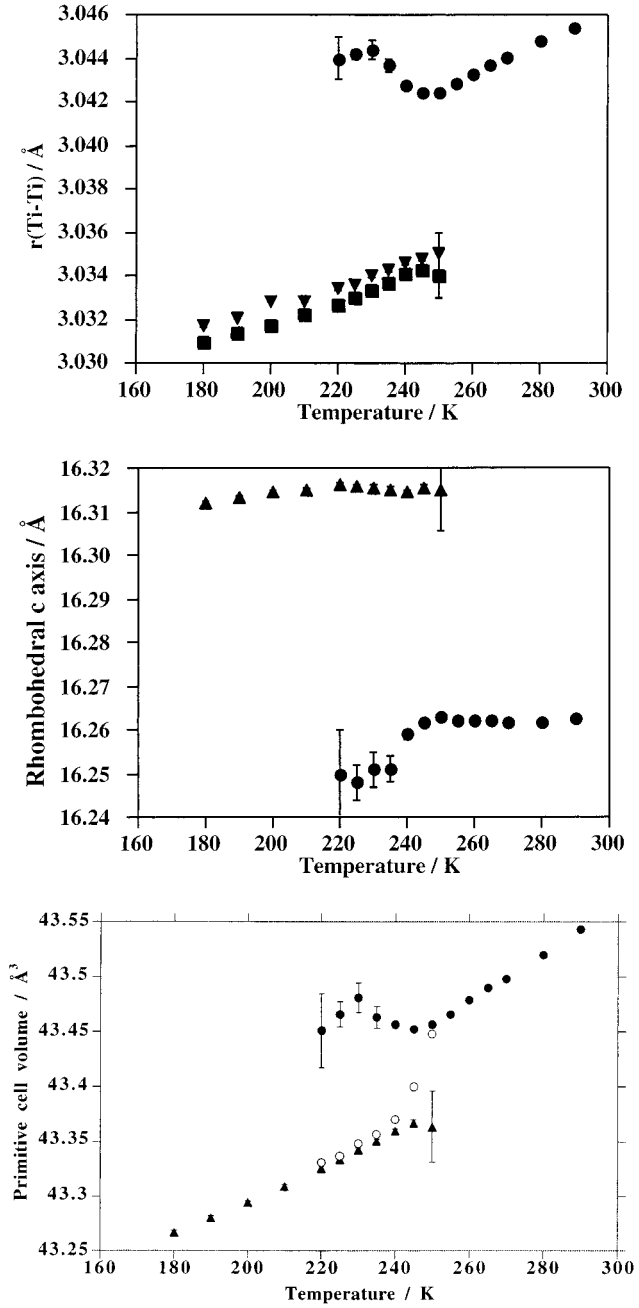

Figure 6. (a, top) Ti−Ti distances in sample 2 ($Na_{0.99(2)}TiO_2$) as functions of temperature. There is one distance in the rhombohedral structure (filled circles) and there are two distances in the monoclinic structure (filled squares × 4 per Ti and filled triangles × 2 per Ti). (b, middle) The hexagonal *c* axis in the rhombohedral phase (circles), and its equivalent in the monoclinic phase ($3c_{mon}$ sin β) (triangles) plotted as functions of temperature. These distances are equivalent to the thickness of three TiO and three NaO slabs. (c, bottom) Primitive unit-cell volume in the two phases as a function of temperature (rhombohedral = circles; monoclinic = triangles). The discontinuous drop at the phase transition is a result of the decrease in Ti−Ti distance. The mean volume, weighted by the mole fraction of both phases, varies smoothly, and is designated by the open circles.

phase transition should not be viewed as a continuous change in the Ti−Ti distance of one single phase accompanying a change in symmetry, but instead as a continuous increase in the fraction of one phase at the expense of the other. The biphasic behavior in the 220−250 K region did not show any hysteresis to a temperature resolution of 5 K when measured by both warming and cooling through the transition. In the region of the phase transition there are insufficient data to enable us to draw detailed conclusions regarding thermal parameters.

We now turn to the details of the symmetry reduction with respect to the two metal sites. The NaO_6 units almost maintain their perfect trigonal antiprismatic geometry (O−Na−O angles change by about 0.05%), but the Na−O bond lengths decrease by about 0.25%, producing the contraction of the NaO slabs. In contrast there is an increase in the thickness of the TiO slabs of about 1.2%; this represents a significant *decrease* in the trigonal compression of the TiO_6 units, which would make them more like regular octahedra if they did not simultaneously distort to 2/*m* symmetry. The distortion of the TiO_6 units is shown diagramatically, and in exaggerated form, in Figure 7, for the results of single-phase refinements at 298 and 5 K, and graphically in Figure 8. The monoclinic distortion corresponds to a lengthening of a pair of Ti−O bonds (shaded in Figure 7) or a slipping of adjacent planes of O atoms relative to one another. O−Ti−O angles change by about 0.5% and on average become closer to 90°. The six identical Ti−O bonds change to a pair lengthened by about 1.5% and four shortened by about 0.5%. In the monoclinic phase, there is still only one crystallographically distinct atom of each type in the primitive unit cell, and there is no suggestion that discrete Ti−Ti bonded clusters are formed. The thermal displacement parameters at 5 K do not suggest a large amount of static disorder which would result from disordered Ti−Ti bonded clusters.

Sample 3 showed behavior similar to that of sample 2, and its Bragg peaks remained about 20% broader than those of sample 2 at all temperatures. The coexistence of rhombohedral and monoclinic phases in sample 3 persisted over a slightly larger temperature range (210−245 K) than in sample 2. The corresponding Ti−Ti separations in samples 2 and 3 differ by about 0.03% or 0.001 Å at each temperature, which equals about 30 standard deviations in the lattice parameters. Consideration of reproducibility of temperature and instrumental calibration indicates that this is not an artifact of performing two different diffraction experiments. The difference in the two samples is much smaller than the range of Ti−Ti distances of about 0.04 Å reported in nominal samples of $NaTiO_2$ and shows that it is possible to produce material of a fairly reproducible nature providing care is taken to avoid Na loss. However, it seems likely that the range of lattice parameters that we observe in our samples is indicative of slight differences in stoichiometry and of Na/Ti disorder, which cannot be resolved using the present diffraction methods.

We have previously reported[15] the results of high-resolution synchrotron X-ray diffraction experiments that allowed us to refine the occupancy of the Na site, assuming the Ti and O sites to be fully occupied and determine the relationship of x in Na_xTiO_2 ($0.9 < x \leq 1.0$) with the lattice parameters a, c, and V. Using high-resolution data and good counting statistics, we were able to refine the occupancy very precisely (esd $\approx$ 0.5%). As stated above, the accuracy in the refined occupancy using either X-ray or neutron diffraction is intrinsically poorer than the statistical precision due to systematic

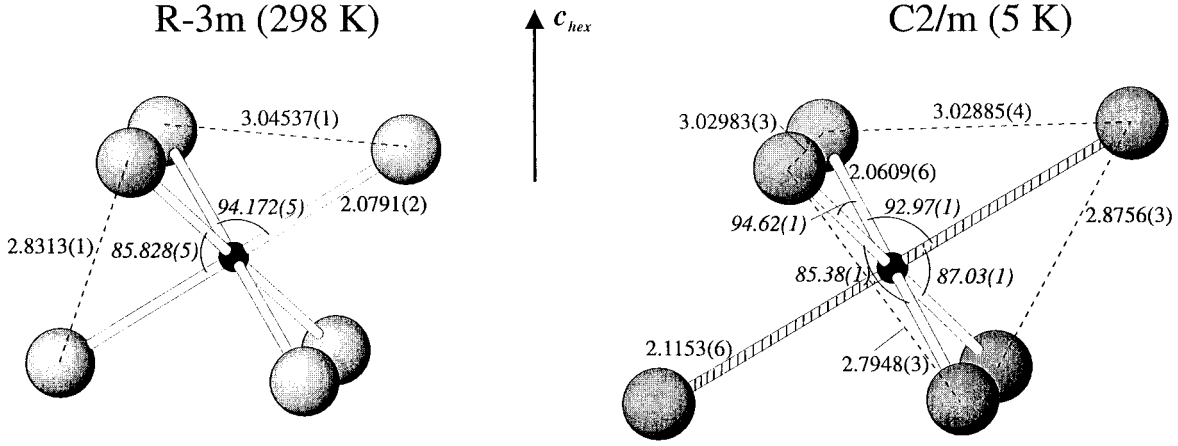

Figure 7. TiO_6 trigonal antiprisms showing the effects of the rhombohedral-to-monoclinic distortion. The distortion, which corresponds to a stretching of the shaded bonds, has been exaggerated. The bond lengths in Å and angles in degrees are those determined at 298 and 5 K, respectively, because these values were determined with the greatest precision.

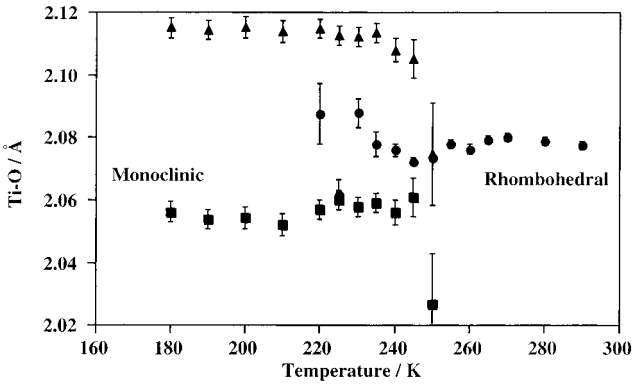

Figure 8. Variation of the Ti−O distances in sample 2 as a function of temperature (rhombohedral = filled circles; monoclinic = filled triangles × 2 bonds per metal; filled squares × 4 bonds per metal).

errors in determination of absorption (particularly important for X-rays) and the strong correlation between the thermal parameters and the site occupancies. In contrast to some of the structural parameters, one can determine the lattice parameters to a very high degree of both precision and accuracy with negligible correlation with other parameters from high-resolution diffraction data. Time-of-flight powder neutron diffraction is particularly good because there is effectively no zero-point correction due to the fixed detector geometry. One can thus readily distinguish different samples on the basis of their lattice parameters. In $NaTiO_2$, these small differences probably indicate very small variations in the Na content of the phases that are inaccessible through refinement of the structure. The higher the Na content, the greater is a (the Ti−Ti distance) and the smaller is c (the average interlayer separation), and the greater is the volume, V. The results of our synchrotron measurements on three different samples shown in Table 4 indicate that a 1 $Å^3$ increase in V represents an increase of 0.056(5) in x. Two of these samples are very similar in refined composition and lattice parameters. We assume that composition is linear with unit-cell volume in the range $Na_{0.9}TiO_2$ to $Na_{1.0}TiO_2$. From this analysis, we infer that samples 1 and 3 are more Na rich than sample 2 by approximately 0.018 and 0.005 in x respectively, differences in composition which cannot reliably be distinguished by refinement of the

Table 4. Correlation of Cell Parameters with Composition Refined from Synchrotron X-ray Powder Diffraction Data[a]

	sample		
	A	B	C
a, b/Å	3.04375(2)	3.04358(3)	3.01358(2)
c/Å	16.2587(1)	16.25329(2)	16.4097(2)
V/Å^3	130.447(2)	130.389(3)	129.061(2)
x in Na_xTiO_2	1.004(3)	0.988(4)	0.922(5)

[a] Note that samples A and B are very similar. The statistical errors in the Na occupancy are probably an underestimate. The thermal parameters for each different atom type were fixed constant at average values to enable the value of x in different samples to be compared: U_{Na} = 0.011 Å,^{2} U_{Ti} = 0.0070 Å,^{2} U_O = 0.0091 Å.^{2}

structure. Different degrees of Na/Ti disorder will also contribute to differences in lattice parameters.

Magnetic Susceptibility Measurements. Measurement of the magnetic moment of each sample as a function of field at room temperature revealed the presence of a tiny amount of a ferromagnetic impurity (probably adventitious Ni or Fe) which was saturated by about 0.8 T. Hence we made temperature-dependent measurements at fields of both 1 and 2 T in order to determine the true value of the paramagnetic susceptibility ($\chi = M(2T) - M(1T)$). The measured susceptibility was corrected for the diamagnetism due to the gelatine capsule and for core diamagnetism. Such corrections are essential as the susceptibility of the sample is relatively small. Plots of the molar magnetic susceptibility of samples 1 and 2 as functions of temperature are shown in Figure 9. The magnetic susceptibility, χ, of sample 2 at 300 K is 4.7×10^{-4} emu mol^{-1} and is only weakly temperature dependent above 250 K. Between 250 and 200 K, which is exactly the region of the structural transition, the susceptibility falls to less than 60% of its room-temperature value, then remains roughly constant to 100 K, and rises in a Curie tail at lower temperatures. The susceptibility does not obey the Curie−Weiss law in any region of the temperature range investigated, but it is possible to fit the data below 150 K to the form $\chi = \chi_0 + C/T$ where C is a Curie constant and χ_0 is the temperature-independent susceptibility below the transition. For sample 2, χ_0 is $2.30(4) \times 10^{-4}$ emu mol^{-1} and C corresponds to a level of about 5% $S = {}^1/_2$ paramagnetic impurities/mol of Ti.

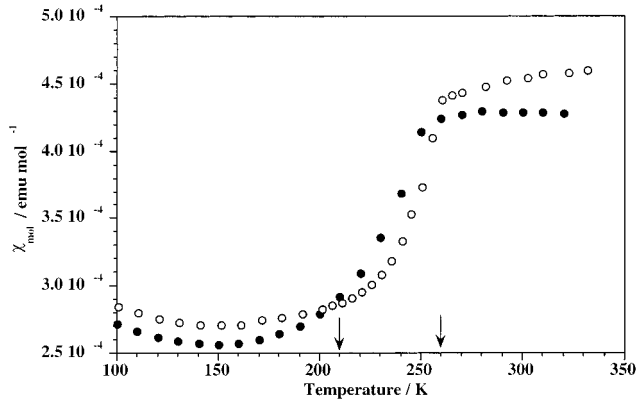

Figure 9. Magnetic susceptibility measured as a function of temperature for sample 1 (filled circles) and sample 2 (open circles) in the region of the transition. Corrections were made for the diamagnetism of both the gelatine sample holder and the atomic cores. The region between the two arrows is that in which 2-phase behavior was observed by neutron diffraction on sample 2.

We investigated the possibility of spin glass behavior resulting from the competition between frustrated antiferromagnetic in-plane exchange and ferromagnetic exchange between Ti ions in the TiO and NaO slabs. This would be similar to the case in $LiNiO_2$.[23] We performed a series of zero-field-cooled (ZFC) and field-cooled (FC) measurements at fields of 0.005 and 0.02 T on a sample containing no measurable ferromagnetic impurity. There was no difference between the ZFC and FC measurements, which rules out behavior similar to that in $LiNiO_2$.

EPR Spectroscopy. A very broad resonance was observed at 295 K. This could only be fit reliably to a single Lorentzian shape below about 100 K where the line width was about 3000 G. The intensity of the resonance measured between 4 and 100 K indicated Curie type behavior, but calibration with an anhydrous copper sulfate standard indicated that only about 5% of the Ti^{3+} ions were contributing to the signal. The *g* value of 1.96, determined by calibration against a DPPH standard, is consistent with Ti^{3+} in a trigonally distorted octahedral environment, and we presume that only the few Ti^{3+} ions in the Na planes contribute to the signal and the other electrons which are delocalized in the Ti planes give only a very broad background signal, characteristic of a metal.

Resistivity Measurements. The samples are all fine powders, and attempts to sinter them at high temperatures inevitably led to a loss of Na, so we have not made temperature-dependent resistivity measurements. We measured the resistivity at room temperature of a cold-pressed pellet of $NaTiO_2$ powder which had been made in the same manner as sample 1 and then washed thoroughly with anhydrous liquid ammonia to ensure that it did not contain any excess Na from the reaction. The measured resistivity was 4 Ω cm. This is only an order of magnitude greater than for metallic $LiTi_2O_4$, which has a room-temperature resistivity of about 0.1 Ω cm for a *sintered* pellet.[24] Considering the unsintered nature of our sample and the fact that a pressure of less than 1 kbar was used for compression, the material appears to be moderately conducting. Hirakawa et al.[12] state that $NaTiO_2$ is insulating at 100 K but conducting at room temperature. However, their sample is highly Na-deficient judging by the hexagonal lattice parameters of $a = 3.001$ Å and $c = 16.44$ Å measured at 1.4 K, which suggest a composition of about $Na_{0.9}TiO_2$, and the lack of any transition in the susceptibility.

(24) Johnston, D. C. *J. Low Temp. Phys.* **1976,** *25*, 145.

Discussion

We have been able to prepare samples of Na_xTiO_2 with *x* approaching 1 by avoiding the loss of sodium in the high-temperature synthesis through low-temperature postsynthetic equilibration with sodium or the use of a controlled excess of sodium. The lattice parameters, when determined precisely, are very sensitive indicators of the sodium concentration in this composition range. The samples with the largest Na concentrations have the shortest interlayer separation and the longest Ti−Ti distances. The high-resolution diffraction measurements show that as the sodium concentration approaches 1.0, there is increased strain within the single-phase samples followed by phase separation in the sample with the smallest *c* and largest *a*. The inhomogeneity that produces the phase separation is also a candidate for the strain broadening and is either attributable to fluctuations in sodium concentration or Na/Ti ordering. Our X-ray and neutron diffraction measurements at room temperature and 5 K showed that a single-phase sample with composition $Na_{0.99(2)}TiO_2$ could be refined, with any suitable set of assumptions about parameter relationships, to give nonzero Na/Ti disorder over the two distinct octahedral sites. The extent of this disorder can be represented as $3.5 \pm 1.5\%$ by considering the *spread* of values determined by the different techniques to reflect the accuracy of the determination. The most precise determination is probably the 5 K neutron refinement where there is least thermal motion and the Na/Ti contrast is stronger than in the X-ray case. The occurrence of Ti^{3+} ions within the NaO slabs is quantitatively consistent with the size of the Curie tail observed in the EPR and low-temperature susceptibility data, because the Ti^{3+} cations present in the NaO slabs should behave as isolated paramagnetic ions.

The peak-shape parameters for sample 3 suggest that the excess broadening results from enhanced strain in this sample compared with the lower sodium content sample 2. The refinements on the biphasic sample 1, where the inhomogeneity is sufficient to produce macroscopic phase separation, indicate, though not definitively, that the extent of Na/Ti disorder may be the factor that differentiates between the two phases and produce the enhanced peak widths observed for sample 3. Sodium concentration gradients are an alternative explanation for the broadening and phase separation, although there is less evidence for these in the biphasic sample.

The monoclinic distortion of the room-temperature structure on cooling below 250 K corresponds to the slippage of adjacent planes of O^{2-} anions relative to one another. Inspection of the bond lengths at the Na and Ti sites demonstrates that the origin of the structural change lies in the Ti−O slabs. There is a sharp intralayer contraction due to an increase in Ti−Ti

bonding (the change in Ti−Ti distance, averaged over the full range of the transition, outstrips the change expected from thermal expansion by about a factor of 6). The thickness of the TiO slabs increases in response to this, and the lengthening of some of the Ti−O bonds lowers the symmetry to monoclinic. The temperature range for coexistence of the rhombohedral and monoclinic phases during the transition appears related to the strain broadening of the Bragg reflections. It seems likely that the phase transition proceeds via a nucleation and growth type mechanism, slow growth being due to the large change in Ti−Ti distance at the transition and pinning of the rhombohedral structure locally by the inhomogeneities that produce the strain broadening.

The broad transition in the susceptibility has been noted previously,[11] and it has been postulated that it accompanies magnetic ordering or freezing of localized Ti^{3+} moments. However our diffraction data suggest that the transition in the susceptibility is intimately associated with a structural change. Also, the shape of the transition, the small size of the susceptibility, and the fact that the major contribution to the susceptibility is temperature independent above and below the transition are more consistent with a transition between two Pauli paramagnetic states with slightly different band structures. Furthermore, while an unfrustrated 2D lattice such as the square lattice can show Neél order above absolute zero if the spins have Ising symmetry,[25] it is not possible to achieve magnetic long-range order in a heavily frustrated lattice such as the triangular lattice.[1] Short-range magnetic ordering in two dimensions produces a broad maximum in the magnetic susceptibility at a temperature determined by the in-plane superexchange.[26] Such a transition can be modeled using a series expansion approach. We were unable to measure the magnetic susceptibility above 330 K due to instrumental constraints, and so it is not possible to fit the data in this way. The data of Takeda et al.[11] were measured up to 400 K with no sign of the susceptibility dropping as would be expected if the feature were due to short-range magnetic ordering. The value of the in-plane exchange constant that would be required by this interpretation is of the order of a few hundred kelvin, which is a plausible value. Our results also show that $NaTiO_2$ cannot strictly be considered a possible model for a truly triangular antiferromagnet with equilateral triangular plaquettes because of the transition from rhombohedral symmetry, with one unique Ti−Ti distance, to monoclinic symmetry with two Ti−Ti distances, as shown in Figure 6a. The lower symmetry lattice based on isosceles triangles would still be frustrated, because it is topologically equivalent to the square lattice with strong next-nearest-neighbor superexchange,[8] but it would not be an ideal model material.

The small susceptibility, the lack of Curie−Weiss behavior, the apparent Pauli paramagnetic behavior above and below the magnetic transition, and the low resistivity are characteristic of a delocalized electron system rather than a paramagnetic insulator. No evidence has been found, from the results of neutron diffraction measurements, for magnetic Bragg peaks indicative of long-range magnetic ordering, or diffuse scattering indicative of short-range magnetic ordering, although such scattering would be very weak in such a low moment system. $LiNiO_2$, also once considered a candidate for showing RVB behavior,[27] *is* an insulating magnet, but it shows spin glass behavior[23] accompanied by Li/Ni disorder of about 3% and competing antiferromagnetic and ferromagnetic exchange, instead of an exotic magnetic ground state. The details of the crystal and electronic structures of $LiNiO_2$ are quite different from those of $NaTiO_2$, as the nickelate retains $R\bar{3}m$ symmetry at all temperatures. There was no evidence for spin glass behavior in $NaTiO_2$. One expects $LiNiO_2$ to be much closer to the insulating condition than $NaTiO_2$, because of poorer *d*-orbital overlap in the former case. The Ti−Ti distance in $NaTiO_2$ is equal to the lattice parameter a in the space group $R\bar{3}m$. In the various $NaTiO_2$ phases we have investigated this is close to the value of about 3.02 Å which is viewed by Goodenough[28] as being the critical distance determining localization or delocalization of d electrons in Ti^{3+} oxides with edge-sharing octahedra. It thus seems likely that $NaTiO_2$ is always in the metallic regime.

Takeda et al.[11] have prepared a sample which has very similar lattice parameters ($a = 3.04$ Å, $c = 16.25$ Å) to our reliably stoichiometric sample 2. Their sample also shows very similar magnetic behavior to our sample, and they presented preliminary data[29] that also showed a rhombohedral-to-monoclinic transition on cooling, although no lattice parameters were given. Their measurement of the specific heat[11] enables us to calculate a value for the entropy change at the transition of about 7 J K^{-1} mol^{-1}. The entropy change for *complete* (i.e. long range) antiferromagnetic ordering of $S = {}^1/_2$ spins should be $R \ln(2S + 1) = R \ln 2 = 5.8$ J K^{-1} mol^{-1}, which is *less* than that measured, further evidence that the material is not an insulating magnet. The density of states at the Fermi level, $n(E_F)$, is proportional to the magnetic susceptibility. The change in $n(E_F)$ at the transition enables us to calculate a value of 8.3 J K^{-1} mol^{-1} for the electronic entropy change of Takeda et al.'s sample using their susceptibility data and assuming metallic states both above and below the transition. This is consistent with the entropy change from the specific heat measurement.

The value of $n(E_F)$ calculated using a free electron model with an electron density of 2.31 electrons/100 Å^3 and taking degeneracy into account was about 5% of the value calculated from the measured susceptibility. This indicates a Stoner enhancement factor for the susceptibility of about 2, which implies narrow bands and the importance of interelectron repulsion, as expected, and is similar to the values found in other early transition metal oxides such as V_2O_3.[30] There is a fairly good correlation, shown in Figure 10, between the Ti−

(25) Mermin, N. D.; Wagner, H. *Phys. Rev. Lett.* **1966**, *17*, 1133.
(26) Navarro, R. In *Magnetic Properties of Layered Transition Metal Compounds*; de Jongh, L. J., Ed.; Kluwer Academic Publishers: Dortrecht, 1990.
(27) Hirakawa, K.; Osborn, R.; Taylor, A. D.; Takeda, K. *J. Phys. Soc. Jpn.* **1990**, *59*, 3081.
(28) Goodenough, J. B. *Prog. Solid State Chem.* **1971**, *5*, 1.
(29) Kakurai, K.; Takeda, K.; Nakajima, K.; Kamiyama, T.; Asai, S. *ISSP Rep.* **1994**, 68.
(30) Tsuda, N.; Nasu, K.; Yanase, A.; Siratori, K. *Electronic Conduction in Oxides*; Springer-Verlag: Berlin, 1983.

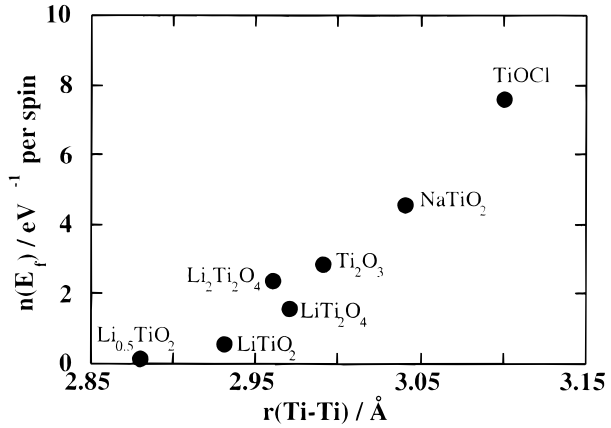

Figure 10. Correlation between Ti−Ti distance between edge-sharing TiO_6 octahedra and the density of states at the Fermi level calculated from susceptibility data for several Ti^{3+} or $Ti^{3+/4+}$ oxides.

Ti separation and $n(E_F)$, calculated from experimental susceptibility data, for the following Ti^{3+} systems with edge-sharing TiO_6 octahedra: disordered rock-salt $LiTiO_2$,[31] spinels $LiTi_2O_4$[32] and $Li_2Ti_2O_4$,[16] stuffed anatase $Li_{0.5}TiO_2$,[32] and Ti_2O_3,[33] which lends support to the metallic interpretation.

In the rhombohedral phase, the trigonal compression of the TiO_6 octahedra lifts the degeneracy of the t_{2g} orbitals and produces a lower a_1 band and an e_π band directly above it (the symmetry labels of the bands refer to their symmetry with respect to the surrounding O atoms). The two bands should overlap as the energy separation will be small. The a_1-e_π separation is probably of the order of the 0.4−0.5 eV calculated for $LiTi_2O_4$[34] which has TiO_6 trigonal antiprisms which are distorted to a similar degree to those in $NaTiO_2$, albeit in the opposite sense (elongated along the trigonal axis). Edwards et al.[34] find that in $LiTi_2O_4$ the trigonal distortion is not sufficient for the separation of the a_1 and e_π components to exceed the width of the t_{2g} manifold. The situation is probably similar in $NaTiO_2$, even though there must be slightly poorer overlap because the Ti−Ti separation is about 2% larger than that in $LiTi_2O_4$. Our structural investigation indicates that at all temperatures there is one d electron in the primitive unit cell of $Na_{1.0}TiO_2$. So the material must be metallic unless it is a Mott−Hubbard or Anderson insulator. The former possibility seems to be ruled out by the behavior of the magnetic susceptibility and the relatively high conductivity. The small amount of disorder in the material and the half-filled nature of the a_1 band rule out Anderson localization. Our picture of the behavior is as follows: at all temperatures, overlap between the Ti^{3+} ions is sufficient for the electron to be delocalized in the narrow conduction band, and the material is metallic. On cooling, thermal contraction precipitates a cooperative increase in Ti−Ti bonding which drives the transition to the lower temperature, and in this case monoclinic, phase which remains metallic. This greater Ti−Ti overlap leads to the shortening of the Ti−Ti distance and expansion of the thickness of the TiO slabs. There is thus a broadening of the conduction band with a concomitant decrease in $n(E_F)$, which produces the transition in the susceptibility. High-level band structure calculations are now required to quantitatively investigate the electronic structure in the two symmetries.

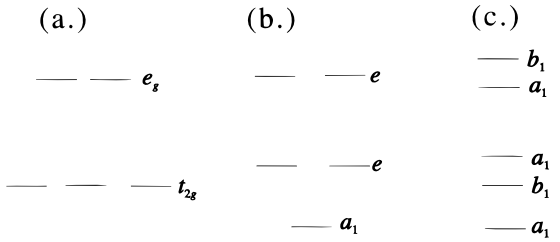

Figure 11. Simple band picture for the t_{2g} manifold of (a) regular octahedron ($m3m$), (b) compressed trigonal antiprism ($\bar{3}m$), and (c) axially distorted compressed trigonal antiprism ($2/m$).

Loss of compression of the trigonal antiprisms below the transition must be accompanied by a decrease in the separation between the a_1 and e_π bands, which would be degenerate if the coordination were a regular octahedron. The picture is further complicated by the lowering of the symmetry of the TiO_6 units from $\bar{3}m$ (D_{3d}) to $2/m$ (C_{2h}) which accompanies the loss of compression. This completely lifts the degeneracy of the original t_{2g} manifold producing two a_1 and one b_1 bands. The structural distortion to monoclinic symmetry in $Na_{1.0}TiO_2$ is very small, but our data clearly show that it originates in the TiO slabs and that it probably therefore has an electronic origin. An attractive interpretation is as follows. The increase in Ti−Ti bonding leads to shorter Ti−Ti distances and a loss of compression of the TiO_6 trigonal antiprisms. This changes the relative energies of the components of the octahedral t_{2g} manifold, such that if a distortion from rhombohedral to monoclinic symmetry takes place there is significant mixing between the two a_1 components of the t_{2g} manifold which lowers the energy of the system (Figure 11). Thus a second-order Jahn−Teller distortion is precipitated by the changes in Ti−Ti bonding, and the result is that the Ti−Ti bonds become inequivalent and the trigonal antiprism distorts. It seems unlikely that the change in symmetry has only an indirect electronic origin and merely represents the packing response of the TiO slabs to the changes in Ti−Ti bond lengths. The distortion of the structure away from rhombohedral symmetry is not required by the changes in bonding, because the shortening of the Ti−Ti distances could be achieved by simply keeping the Ti−O bond lengths equal and decreasing the compression of the trigonal antiprisms. Indeed, the stabilization conferred by the adoption of monoclinic symmetry is reduced as the Ti oxidation state increases and material which is 7% deficient in Na does not become monoclinic.[13] We should examine whether this Jahn−Teller mechanism is consistent with the behavior of other AMO_2, as described by Delmas et al.[35] Phases with non-Jahn−Teller transition metal cations crystallize with the ideal

(31) Lecerf, A. *Ann. Chim.* **1962**, *7*, 513
(32) Cava, R. J.; Murphy, D. W.; Zahurak, S. M.; Santoro, A.; Roth, R. S. *J. Solid State Chem.* **1984**, *53*, 64.
(33) Mott, N. F. *J. Phys. Colloq.* **1981**, *42*, 277.
(34) Edwards, P. P.; Egdell, R. G.; Fragala, I.; Goodenough, J. B.; Harrison, M. R.; Orchard, A. F.; Scott. E. G. *J. Solid State Chem.* **1984**, *54*, 127.
(35) Delmas, C.; Fouassier, C.; Hagenmuller, P. *Phys. B* **1980**, *99*, 81.

ordered rock-salt structure in the space group $R\bar{3}m$ at all temperatures, e.g., $NaCoO_2$[36] (d^6) and $NaCrO_2$[37] (d^3). However, $NaMnO_2$[38] never adopts this structure and the high-spin Mn^{III} d^4 ions are always strongly (first order) Jahn−Teller distorted. α-$NaMnO_2$ adopts the space group $C2/m$ and is isostructural with the monoclinic form of $NaTiO_2$ described here. The distortion in the Mn case is much greater with four Mn−O bonds of 1.97 Å and two of 2.33 Å. Above 850 °C, the transition to β-$NaMnO_2$ ($Pmmn$) maintains the distortion (four bonds of 2.13 Å and two of 2.38 Å). $NaNiO_2$[39] (d^7) undergoes a transition, on warming, from $C2/m$ to $R\bar{3}m$ at about 400 °C. This behavior is reminiscent of $NaTiO_2$, although the Jahn−Teller distortion is again large and first order like in $NaMnO_2$. We and others[14] find no evidence for distortion in $NaTiO_2$ on deintercalation of Na as is found in α-$NaFeO_2$.[40] In fact, the $R\bar{3}m$ symmetry seems to be reinforced[13] in line with the removal of potentially Jahn−Teller-active Ti^{3+}.

The interpretation of the phase transition in $NaTiO_2$ as arising from extended metal−metal bonding combined with a local distortion can be considered in relation to other early transition metal oxides. There are important differences from the well-known insulator to metal transition on warming from 400 to 600 °C in Ti_2O_3[33,41−43] with the corundum structure. Ti_2O_3 crystallizes in $R\bar{3}c$ (No. 167), and the presence of the glide operation results in an even number of Ti^{3+} (four), and hence valence electrons, in the primitive unit cell, allowing explanations based on the formation of a band insulator. The Ti−Ti distance between edge-sharing TiO_6 trigonal antiprisms in Ti_2O_3, changes by about the same amount as in $NaTiO_2$ at the transition, but in the opposite sense, i.e., it decreases on warming indicating greater bonding at higher temperatures. In Ti_2O_3 there is also much more important Ti−Ti bonding via face-shared trigonal antiprisms, which decreases on warming. The two effects mean that the structural phase transition[43] in Ti_2O_3 has a greater effect on the band structure than in $NaTiO_2$. At low temperatures the a_1 conduction band, corresponding to Ti−Ti bonding between face-sharing trigonal prisms, does not overlap with the e_π band above it corresponding to Ti−Ti bonding between edge-sharing trigonal prisms. The two a_1 bands are filled by the four electrons in the primitive unit cell, and the material is an insulator. At higher temperatures, the structural changes dominated by the weakening of the face-shared Ti−Ti bond cause the a_1 and e_π bands almost,[41] or actually,[42] to overlap producing a narrow-bandgap p-type semiconductor or a metal. So the details of the behavior in Ti_2O_3 are quite different from those of $NaTiO_2$.

$Li_{0.7}VO_2$[44−47] is isostructural with $NaTiO_2$ but has Li vacancies and mixed valence $V^{3+/4+}$ character. It goes through an apparently fairly similar transition in the susceptibility to that of $NaTiO_2$ between 400 and 500 K. The susceptibility is almost flat above the transition. The lattice parameters change at the transition in a fashion similar to those in $NaTiO_2$, but the effect is almost an order of magnitude larger in $Li_{0.7}VO_2$. The transition has been associated with a semiconductor-to-metal transition, driven by changes in V−V bonding, on warming. At high temperatures, the V−V distances are all equal and below the critical distance for delocalization (2.90 ± 0.01 Å) determined by Goodenough et al.,[28] so the electrons are itinerant and the material is metallic. Below the transition, weak superstructure reflections indicate a lowering of symmetry[45,46] with the formation of triangular V_3 units with V atoms displaced by about 0.1 Å[46] from their ideal positions, which is much greater than the displacements in $NaTiO_2$. The distortion has been rationalized by Pen et al.[48] in terms of orbital ordering and by Goodenough et al.[47] in terms of the lattice instability associated with proximity to the localized−delocalized critical V−V separation. The changes in the structure and the susceptibility at the transition are, as well as being much larger than those in $NaTiO_2$, of a different type. TiOCl and TiOBr[49] have received some attention as possible RVB materials on the basis that they are Mott insulators (brown in color unlike black $NaTiO_2$) with nearest-neighbor Ti−Ti separations, across a shared octahedral edge composed of two O atoms, of 3.10 and 3.19 Å, respectively. There is the possibility of magnetic frustration on the rectangular lattice via next-nearest-neighbor superexchange interactions. The magnetic susceptibility is flat between 100 and 300 K, about double that of $NaTiO_2$ and smaller than expected for a magnetic insulator which is ascribed[49] to the moment reduction expected in an short range ordered $S = {}^1/_2$ state. A comparison of TiOCl and TiOBr[49] with other materials of interest concludes that these are clearly more localized than $NaTiO_2$ and must be closer to being good models for frustrated $S = {}^1/_2$ antiferromagnets.

Conclusions

We have explored the difficulties associated with the preparation of reliably stoichiometric and single-phase $NaTiO_2$. Prolonged equilibration with Na vapor produces single-phase material with a stoichiometry close to $Na_{1.0}TiO_2$. High-resolution neutron powder diffraction shows that the transition observed in the magnetic susceptibility is a structural phase transition driven by changes in Ti−Ti bonding. Inhomogeneity, in either the sodium distribution or, more likely, the small Na/Ti disorder seen in both diffraction and magnetic measure-

(36) Fouassier, C.; Matejka, G.; Reau, J.-M.; Hagenmuller, P. *J. Solid State Chem.* **1973**, *6*, 532.
(37) Miyazaki, S.; Kikkawa, S.; Koizumi, M. *Rev. Chim. Miner.* **1982**, *19*, 301.
(38) Parant, J.-P.; Olazchaga, R.; Devalette, M.; Fouassier, C.; Hagenmuller, P. *J. Solid State Chem.* **1971**, *3*, 1.
(39) Dyer, L. D.; Borie Jr., B. S.; Smith, G. P. *J. Am. Chem. Soc.* **1954**, *76*, 1499.
(40) Takeda, Y.; Nakahara, K.; Nishijima, M.; Imanishi, N.; Yamamoto, O.; Takano, M.; Kanno, R. *Mater. Res. Bull.* **1994**, *29*, 659.
(41) Mott, N. F. *J. Phys.* **1981**, *42*, 277.
(42) Zeiger, H. J. *Phys. Rev.* **1975**, *B11*, 5132.
(43) Rice, C. E.; Robinson, W. R. *Acta Crystallogr.* **1977**, *B33*, 1342.
(44) Hewston, T. A.; Chamberland, B. L. *J. Solid State Chem.* **1986**, *65*, 100.
(45) Hewston, T. A.; Chamberland, B. L. *J. Solid State Chem.* **1985**, *59*, 168.
(46) Cardoso, L. P.; Cox, D. E.; Hewston, T. A.; Chamberland, B. L. *J. Solid State Chem.* **1988**, *72*, 234.
(47) Goodenough, J. B.; Dutta, G.; Manthiram, A. *Phys. Rev.* **1991**, *B43*, 10171.
(48) Pen, H. F.; van den Brink, J.; Khomskii, D. I.; Sawatzky, G. A. *Phys. Rev. Lett.* **1997**, *78*, 1323.
(49) Beynon, R. J.; Wilson, J. A. *J. Phys.: Condens. Matter* **1993**, *5*, 1983.

ments, affects the electronic properties: samples with greater strain broadening have broader structural transitions with enhanced coexistence ranges for the rhombohedral and monoclinic phases.

The absence of strong temperature dependence in the magnetic susceptibility above or immediately below the transition leads to the conclusion that the behavior of $NaTiO_2$ is similar to that shown by other reduced early transition metal oxides: the d electrons are delocalized, and it is not a candidate material for an exotic frustrated magnetic ground state.

It appears that there are two electronic contributions to the structural and magnetic behavior of $NaTiO_2$. The transition in the magnetic susceptibility is a result of changes in the band structure which are driven by an increase in Ti−Ti bonding (Figure 6a). The Ti−Ti distance is almost equal to the critical value of Good-enough,[28] so it is not unexpected that temperature changes result in electronic and structural changes. The increased Ti−Ti bonding leads to a decrease in the trigonal distortion of the TiO_6 octahedra, thus the a_1 HOMO and the e_π LUMO, both part of the octahedral t_{2g} manifold, become closer in energy. As the two become closer in energy, a distortion to 2/*m* symmetry takes place which lifts the degeneracy of the e_π producing a_1 and b_1 subbands, the former of which can mix with the a_1 HOMO. Thus a second-order Jahn−Teller distortion is precipitated by a change in bonding. The Jahn−Teller distortion has a very small effect on the Ti−Ti distances (about 10% of the *change* in bonding which takes place, which is in turn about 0.3% of the bond length). The Ti−O distances are affected to a larger degree, but the range of Ti−O distances is less than in isostructural materials which exhibit first-order Jahn−Teller distortions.

Acknowledgment. We wish to thank the EPSRC for access to ISIS and the Daresbury Laboratory, and for research grants to M.J.R. and A.H., and the CCLRC and EPSRC for a studentship to A.J.F. S.J.C. wishes to acknowledge the support of the Lloyd's of London Tercentenary Foundation and St Hugh's College, Oxford. We thank Dr D. M. O'Hare (ICL Oxford) for access to the four-zone tube furnace, and Professor F. J. DiSalvo (Cornell University) for useful discussions.

CM970538C